Guedes, A.; et al., 2008: Hybrid - LOW COST, LOW POWER, HIGH SENSITIVITY MAGNETOMETER

A.S. Edelstein*, James E. Burnette, Greg A. Fischer, M.G. Koebke, Kimberly Olver
U.S. Army Research Laboratory
2800 Powder Mill Rd
Adelphi, MD 20783-1197

Shu-Fan Cheng
Naval Research Laboratory
4555 Overlook Ave., S.W.
Washington, DC 20375

William Egelhoff, Jr
Building 223, Room B152
National Institute of Standards & Technology 100 Bureau Dr.
Gaithersburg MD 20899-8552

Prof. Edmund Nowak
Dept. of Physics and Astronomy
University of Delaware
223 Sharp Labs
Newark, DE 19716

ABSTRACT

Because weapon systems, vehicles, and most communication systems all generate magnetic fields, magnetic sensors can provide useful military information. There has been significant recent progress in magnetometry. This progress includes chip scale magnetometers, magnetoelectric sensors, devices with much larger magnetoresistance (MR) and an ARL invention, the MEMS flux concentrator that is needed at low frequencies to take advantage of the larger MR values. In addition, better algorithms using total field measurements have been developed to take advantage of the improved magnetic sensors. Our main topic is the development of the MEMS flux concentrator. The MEMS flux concentrator has the potential to be a factor of 10 cheaper, consume 1% of the power, be a factor of 100 more sensitive at 1 Hz and occupy 0.001 the volume of the magnetic sensor element currently used in Army sensor systems, the Brown flux gate.

1. INTRODUCTION

Magnetic sensors for military applications have the advantage being able to detect through walls and foliage, requiring only a small amount of bandwidth, and being insensitive to weather conditions. Further it is difficult to make a weapons system or send a signal that can not be detected by a magnetic sensor.

There are two basic types of magnetic sensors, vector sensors and total field sensors. Vector sensors measure the field in a given direction. Total field sensors measure magnitude of the magnetic field without regard to direction by measuring the splitting between quantum energy levels. At present, all total field sensors are costly. They have the advantage of being insensitive to the rotational vibrations of moving vehicles. One new approach for making smaller total field sensors is to make ship scale atomic magnetometers. Schwindt et al. (2004) have been able construct a sensor by building a stack which includes lasers, optics, optical cell, and detector into a silicon chip. This stack is shown in Fig. 1. The magnetoelectric magnetometer (Dong, 2005) is a clever arrangement of two magnetostrictive slabs of material surrounding a piezeoelectric slab. In the presence of a field, the magnetostrictive material stresses the piezeioeltectic material which generates a voltage. Thus, the sensor generates an output voltage without drawing power.

Report Documentation Page

Form Approved
OMB No. 0704-0188

1. REPORT DATE	2. REPORT TYPE	3. DATES COVERED
01 DEC 2008	**N/A**	**-**

4. TITLE AND SUBTITLE	5a. CONTRACT NUMBER
Low Cost, Low Power, High Sensitivity Magnetometer	5b. GRANT NUMBER
	5c. PROGRAM ELEMENT NUMBER
6. AUTHOR(S)	5d. PROJECT NUMBER
	5e. TASK NUMBER
	5f. WORK UNIT NUMBER
7. PERFORMING ORGANIZATION NAME(S) AND ADDRESS(ES) **U.S. Army Research Laboratory 2800 Powder Mill Rd Adelphi, MD 20783-1197**	8. PERFORMING ORGANIZATION REPORT NUMBER
9. SPONSORING/MONITORING AGENCY NAME(S) AND ADDRESS(ES)	10. SPONSOR/MONITOR'S ACRONYM(S)
	11. SPONSOR/MONITOR'S REPORT NUMBER(S)

12. DISTRIBUTION/AVAILABILITY STATEMENT
Approved for public release, distribution unlimited

13. SUPPLEMENTARY NOTES
See also ADM002187. Proceedings of the Army Science Conference (26th) Held in Orlando, Florida on 1-4 December 2008, The original document contains color images.

14. ABSTRACT

15. SUBJECT TERMS

16. SECURITY CLASSIFICATION OF:			17. LIMITATION OF ABSTRACT	18. NUMBER OF PAGES	19a. NAME OF RESPONSIBLE PERSON
a. REPORT	b. ABSTRACT	c. THIS PAGE			
unclassified	**unclassified**	**unclassified**	**UU**	**9**	

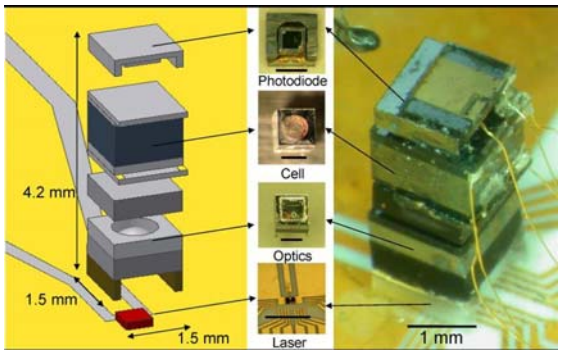

Figure 1. Illustration of the chip scale atomic magnetometer.

There are many kinds of vector magneotmeters that vary greatly in cost and sensitivity. At the low end are hall sensors used extensitvely in automotive applications. At the high end are superconducting quantum interference device sensors SQUID which are used to measure the small magnetic signals from brain. Other types of vector magnetometers are fluxgate, coil based, and magnetoresistance magnetometers. Magnetoresistance devices contain resistive element that change their resistance in the presence of a magnetic field. The maximum percentage change in the resistance as a function of the applied magnetic, denoted as the magnetoresistance (MR), is one important measure of the quality of magnetoresistance sensors.

Above about 5 Hz, coil based have a high sensitivity and they can be used to detect power lines, the operation of electrical equipment, and the transmission of signals. The motion of many objects on the battlefield is sufficiently low that one needs to have sensitivity at frequencies less that one Hz.

The first examples of materials with large MR were spin valves. Spin valves have values of MR of 12% instead of the highest previously observed values of magnetoresistance, 3.5%, obtained in anisotropic magnetoresistance sensors. The 2007 Noble prize in physics was awarded to the discoverers of giant magnetoresistance in spin valves. Values of MR as large as 400% were observe in later work (Parkin, 2004; Yuasa, 2004) on magnetic tunnel junctions with MgO tunnel barriers. In these junctions, the majority electrons have a higher transition probability of tunneling through the barrier than the minority electrons. At present, one can not take full advantage of the large MR of these devices at low frequencies because of the large 1/*f* noise in these devices. The 1/*f* noise is a result of trapping defects in the tunnel barrier of MTJ devices and the thermal instability of the magnetic domains in the soft layer GMR and MTJ devices 9 (Jiang. 2004). Even though anisotropic magnetoresistance sensors have magnetoresistance values less than 3.5% they are often used for low frequency applications because they have less 1/*f* noise than magnetoresistance sensors with larger values of magnetoresistance. Figure 2 shows the sensitivity of a MTJ sensor at high frequencies and illustrates the promise these kind of magnetresistance sensor offers if we could solve the problem of 1/*f* noise. At 500 kHz, the sensor has a detectivity of 2pT/Hz1/2, but the detectivity is much lower at 1 Hz (Chaves, 2008).

Previously (Edelstein, 2002; Edelstein, 2004; Burnette, 2008), we suggested a method for mitigating the problem of 1/*f* noise. We and others (Guedes, 2008) have been utilizing this approach. Here we report the unambiguous validation of the MEMS flux concentrator concept and a clear route for producing magnetic sensors with a detectivity of a few pT/Hz$^{1/2}$ at 1 Hz.

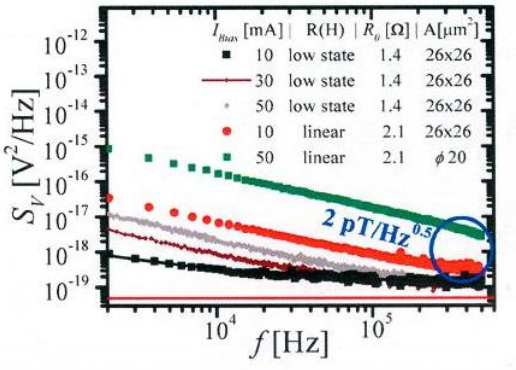

Figure 2. Power spectrum in a magnetic tunnel junction with a MgO barrier (Chaves, 2008).

2. CONCEPT

The concept for dealing with 1/*f* noise in magnetic sensors is illustrated in Fig. 3. In the device, the magnetic sensor is placed between flux concentrators. The spacing between the flux concentrators is 52 microns. Flux concentrators are films of soft magnetic materials that attract

magnetic field lines. Permalloy, an alloy of 80%Ni, 20% Fe is an example of a soft magnetic material. Figure 4 illustrates how the flux lines are attracted to the soft magnetic material in the device. The flux concentrators are deposited on MEMS structures that can be driven to oscillate by electrostatic comb drives. When the spacing between the MEMS structures is small they concentrate the field more than when the spacing is large. Thus, when they are in motion they modulate the field at the position of the sensor. This increases the operating frequency of the sensor to a frequency where $1/f$ noise is much less of a problem.

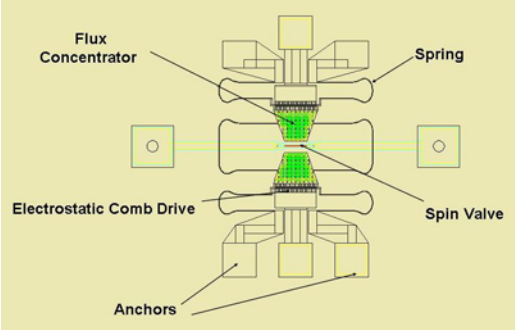

Figure 3. Schematic of the MEMS flux concentrator.

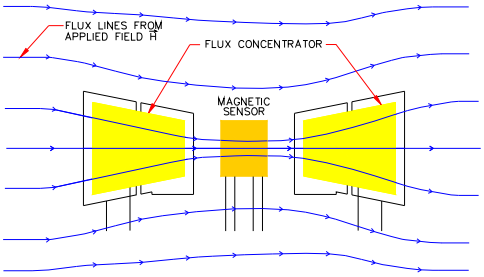

Figure 4. Illustration of the flux concentrator attracting the magnetic flux lines.

3. FABRICATION

The basic problem in utilizing the concept was the difficulty of combining two very different technologies, MEMS technology and magnetic sensor technology. We will separately discuss the fabrication of the MEMS and sensor portions of the device, the problem of combining the two portions, and the solution to this problem.

3.1 MEMS Modeling and Fabrication

The designs of the MEMS structure were checked by using the finite element code Ansys. The calculated characteristics of the designs, such as the normal mode resonant frequencies, were later found to in general agreement with the results of these calculations.

Though we initially started fabricating the MEMS structure by first building up the structure on silicon wafers, it was decided that processing steps could be eliminated by using silicon on insulator (SOI) wafers. It was found that it was necessary to be careful in selecting the company that provided the SOI wafers since the bonding between the device layer and the handle wafer must be very good so that the etch rate of the SiO_2 is isotropic. We used standard optical lithography with two micron resolution. Initially liquid HF was used in the release step but later it was found that using a vapor HF tool increased our ability to control the process and eliminated the problem of delamination of the magnetic film that had been deposited on the MEMS structure. As stated above, the motion was driven by electrostatic comb drives. Electrostatic comb drives are in positions of unstable equilibrium. In the presence of an applied voltage, lateral displacement tends to increase. The Si springs of the MEMS structure prevent the teeth of the comb drive from shorting when the comb drive is energized. Because of this, it is essential to maintain the symmetry and to limit the voltage driving the voltage below the voltage where instability causes shorting. This requires having large anchors that support the released structure that are insensitive to small differences in etch rate over the surface of the wafer.

3.2 Sensor fabrication

We chose to use spin valves as our magnetic sensor because spin valves have considerable $1/f$ noise and are readily available. Spin valves are giant magnetoresistance devices consisting of a four layer structure of two thin ferromagnetic films separated by a thin insulator. The magnetization of one of the ferromagnetic layers is pinned by exchange interactions with the fourth layer, an antiferromagnet. The resistance is a minimum (maximum) when the magnetizations of the two ferromagnetic layers are parallel (antiparallel). The spin valves were fabricated by NVE Corporation and have MR values of about 5 %.

The enhancement of the field due to the MEMS flux concentrators as a function of the separation between the flux concentrators was calculated using a finite element code from Ansoft Corp. The results of these modeling calculations are shown in Fig. 5.

3.3 Problem and Solution in Combining the Technologies

It was found that the final step of the MEMS structure, using HF to remove the SiO_2 and thus allowing the MEMS structure to move, destroyed the spin valves. The damaged spin valve is shown in Fig. 6. Several attempts at finding a suitable protective layer failed. The solution was to not expose the spin valve to HF. This was accomplished by fabricating the HF structure on one chip and the spin valves on another chip. Indium was deposited on the chip containing the spin valve and the two chips were flip chip bonded. The combined chips were packaged and wire bonded. Figure 7 shows an image of the complete packaged device.

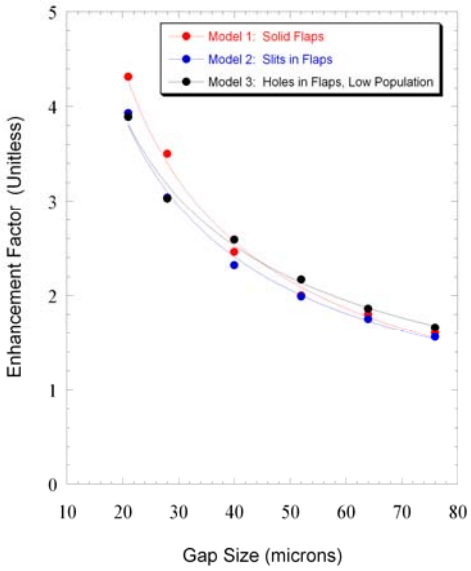

Figure 5. Results of the modeling the enhancement of the field due to the flux concentrators as a function of the separation between the flux concentrators.

4. TESTING

In discussion with other researchers, the question arose as to whether adding the flux concentrator would add to the 1/*f* noise. If it did, then there would be no reason to continue the project. To answer this question, similar samples were prepared with and without flux

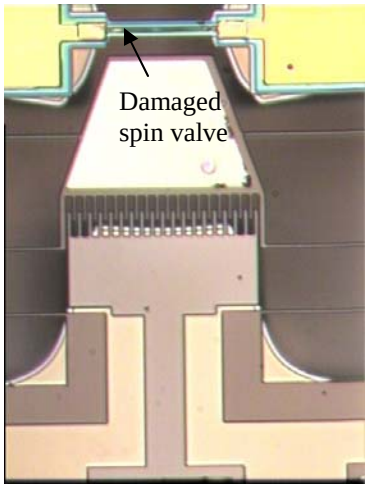

Figure 6. Device showing the damage to the spin valve by immersion in HF.

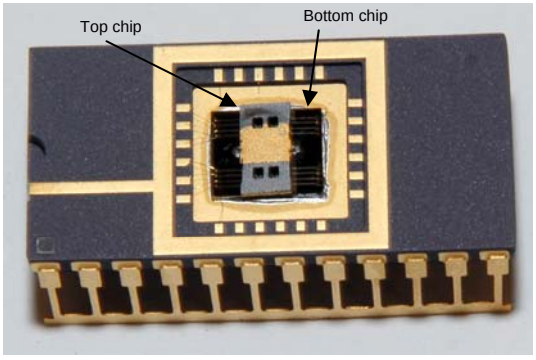

Figure 7. Example of a complete Device

concentrators. It was found that the noise was the same with and without flux concentrators, i.e., flux concentrators do not increase the noise. The reason for this is that the 1/*f* noise is proportional to the reciprocal of the volume and the flux concentrators are much larger than the spin valves.

The different components of the device were tested separately. The electrostatic comb drive of the MEMS structure was driven by a signal generator followed by an amplifier. At atmospheric pressure with our current design to

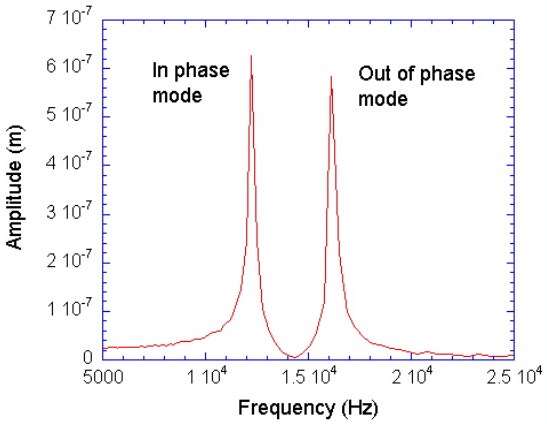

Figure 8. Measured amplitude of the two in plane normal modes as a function of frequency for one of the devices.

obtain a 5 micron amplitude one must drive the MEMS structure with a signal with a 90 volt amplitude. The two MEMS structure on both sides of the sensor that are covered by permalloy are connected by silicon springs. Because of these connecting springs, there are two normal modes for the motion. In one mode, the two structures move so that the separation between the two structures remains constant. We denote this mode as the in phase mode. In the other mode, the separation between the two structures oscillates. We denote this as the out of phase mode. The amplitude of two modes as function of frequency is shown in Fig. 8. The normal mode used in our current design is the out of phase mode in which the spacing between the flux concentrators oscillates. The *Q* of this mode in air is about 30. It takes 90 volts to drive the structure so that the MEMS motion has a 5 micron amplitude in air.

The force provided by the electrostatic comb drives is given by

$$Force = \partial Energy / \partial overlap =$$
$$\varepsilon_o \cdot (n-1) \cdot h \cdot V^2 / 2d \qquad (1)$$

where *d* is the separation between the teeth, *h* is the height of the teeth, n is the number of teeth, and *V* is the voltage applied between adjacent teeth. It is important to note that the force is proportional to V^2. Thus, the drive oscillator frequency is adjusted so that first harmonic is equal to the resonant frequency of the MEMS structure. The MEMS structure was energized using an Agilent 33220A signal generator followed by an amplifier with a gain of 10. A constant current was applied to the spin valve using a battery. The resultant voltage was analyzed using Stanford Research Systems SR640 dual channel low pass filter, a National Instruments BNC 2090 terminal block, and a LabView program that yields the power spectrum. The signal was demodulate using a lock-in amplifier driven at the resonant frequency of the MEMS structure.

Figure 9 shows the magnetoresistance of one of our spin valves. Note it has the necessary characteristics of being linear near zero field and non hysteretic.

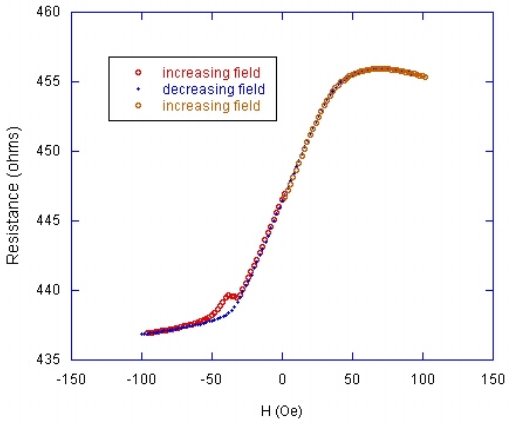

Figure 9. Magnetoresistance of one of the spin valves.

The power spectrum of the output of the spin valves on a device is shown in Fig. 10. One sees the sidebands around the resonant frequency that result from a 25 Hz, 0.22 Oe field. The current through the spin valve was 0.823 mA. Results are shown for three different drive voltage applied to the comb drive. As proof that the sideband were a due to the motion of the MEMS structure, the power spectrum was recorded when the drive frequency was shifted away from the resonant frequency. The off resonance power spectrum is shown in Figl 11. One sees in Fig. that the sidebands are no longer present when MEMS structure is not driven at its resonant frequency. The reason for this is that the amplitude of theof the motion is no longer increased by the *Q* of the resonance. The amplitude of the sidebands in the power spectrum was measure as a function of the amplitude of the AC drive voltage. The results of these measurements are shown in Fig. 12. One sees the amplitude increases as the fourth power of the drive voltage *V*. This is the correct dependence because from Eq. 1 the force is

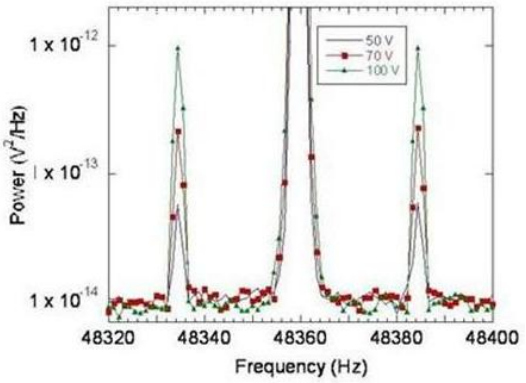

Figure 10. Plot of the power spectrum showing the sidebands around the resonant frequency for three different values of the drive voltage.

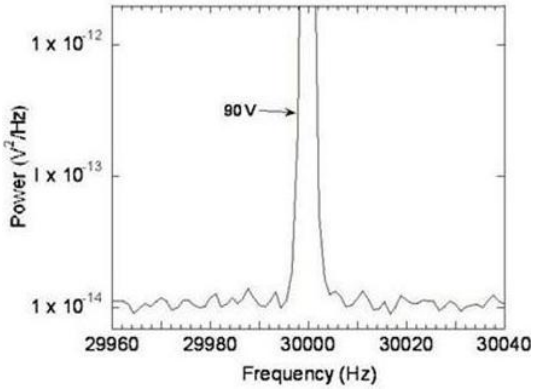

Figure 11. Absence of the sidebands when the drive frequency is not equal to the resonant frequency of the MEMS structure,

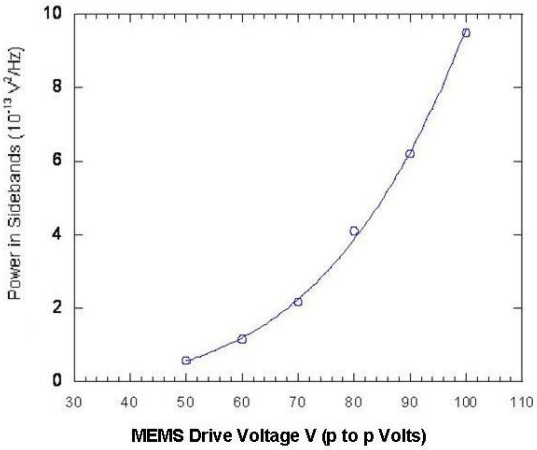

Figure 12. Plot of the amplitude of the sidebands around the resonant frequency versus the voltage driving the MEMS structure. The solid curve is computed from $AV^{4.08}$ where A is a constant.

proportional to V^2. Thus, the amplitude of the motion and the voltage out are also proportional to V^2. The power spectrum is proportional to the square of the output voltage should be proportional to V^4.

Keeping the drive voltage constant, it was found that vacuum packaging increases the *Q* and increases the amplitude of the sidebands. The reason this for this increase is that air resistance is the main energy loss. The Q of many vacuum packaged MEMS devices is as high 20,000 or more. A vacuum sealed device is shown in Figure 13.

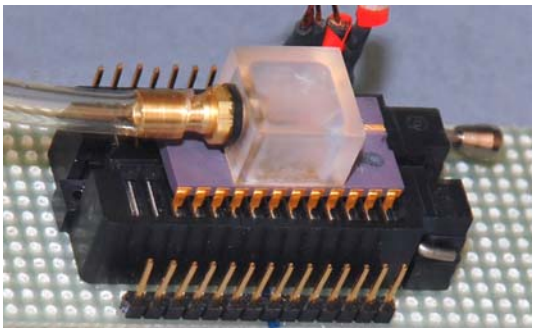

Figure 13. Photograph of a vacuum sealed device.

Our initial results showing the increase in the amplitude of the sideband with decreasing pressure is shown in Fig. 14. On going experiments show that by decreasing the pressure further we can increase the amplitudes of the sidebands by a factor greater than several hundred.

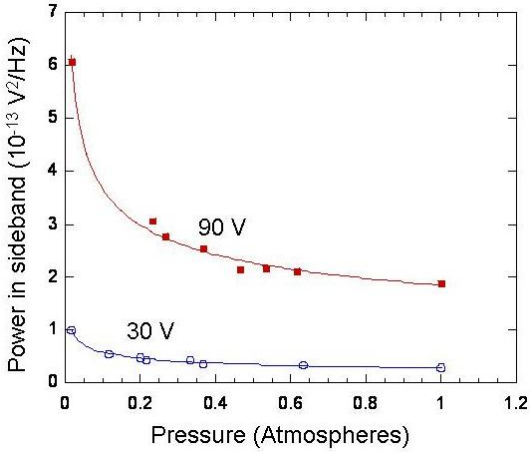

Figure 14. Initial increase of the amplitude of the sidebands with decreasing pressure.

These results prove unambiguously that by modulating the field we have been able to increase the operating frequency of the sensor to a region where the 1/*f* noise is much smaller. We conclude by discussing the present status of the device, its potential, and how this potential can be realized.

5. PRESENT STATUS, POTENTIAL AND REALIZING THE POTENTIAL OF THE DEVICE

The results of tests validate the concept of the MEMS flux concentrator for mitigating the problem of 1/f noise by shifting the operating frequency. Devices have been fabricated that have a sensitivity of 10 nT. This sensitivity is comparable to the sensitivity of commercial sensors. Even with these first working devices, out results extrapolated to 1 Hz show a factor of two improvement in the signal to noise ratio. As will be discussed below, using the MEMS flux concentrator, we will be able to produce a magnetic sensor that will have a detectivity of 5 $pT/Hz^{1/2}$ at 1 Hz.

Table 1 shows a comparison of the expected performance of the MEMS flux concentrator with the magnetometer currently used in Army multimodal sensor systems, the Brown fluxgate. One sees the MEMS fluxgate magnetometer is likely to be a 100 times more sensitive, cost a factor of 10 less to produce, consume about 1 % the power, and occupy 1/1000 the volume.

Figure 15 can be used to estimate the improvement in detection that can be achieved with this better sensitivity. Since the improvement is about a factor of 10^2 to 10^3 over current low cost sensors and the signal from most targets decreases as $1/r^3$, the detection range will be increased by a factor of about 5. It must be pointed out, however, that this improvement can not be achieved without removing the effect of environmental noise. Because much environmental noise is correlated over large distances, its effect can be removed by

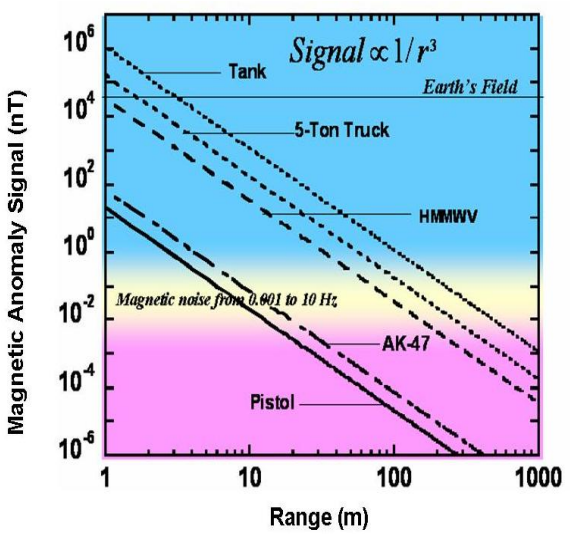

Figure 15. Magnetic signal strength vs. range for several different targets.

taking the difference between the reading of thesensor and a reference sensor that is separated from the sensor by a distance of 20 feet to one km. km. Magnetic anomaly signals smaller than 1 pT have been detected by this technique for removing the effect of enviromental noise.

We now address how one can modify our current design to achieve a detectivity of 5 $pT/Hz^{1/2}$ at 1 Hz and make fieldable sensors. The necessary steps are:

1. Increasing the amplitude of the MEMS motion. This can be accomplished increasing the length of the teeth in the elastic comb drive and vacuum packing of the sensor. The vacuum packaging allows one to achieve the same amplitude for the motion with a much smaller voltage. As pointed out above, one can not use voltages larger than some threshold because of the electrostatic instability of comb drives.
2. Increasing the enhancement of the magnetic field by using a new concept of a compound flux and increasing the modulation of the field by a different MEMS design. Provisional patents have been filed on these new approaches.
3. Using magnetic tunnel junctions instead of the spin valves. Magnetic tunnel junctions have larger MR values than spin valves and can saturated in smaller values of magnetic fields.
4. Sensing the motion and adding feedback so that the MEMS structure automatically operates at the resonate frequency of the MEMS structure. This avoids the necessity

of setting an oscillator on the correct frequency to drive the high *Q* MEMS structure.

6. SUMMARY

We have proven the validity of the MEMS flux concentrator concept for mitigating the serious problems of 1/*f* noise in magnetic sensors and been able to produce a sensor that is comparable to current commercial sensors. Further, we have discussed a realistic, direct path for producing a magnetic sensors that will have increase the detection range by about a factor of 5.

Table 1. Comparison of the MEMS Flux Magnetometer with the Magnetometer Currently Used by the Army, the Brown Flux Gate Magnetometer

Type	Response	Field Noise	Cost Sensor Element	Power Consumption	Size of Sensor Element
MEMS flux Concentrator1st version	0.04%/Oe	0.3nT/rt Hz at 1 Hz	$5	1.6 μW	1 mm3
MEM flux concentrator Later version	1-2%/Oe	0.01nT/rt Hz at 1 Hz	$5	15 mW	1 mm3
Fluxgate Brown	0.8 V/Oe	1.7 nT/rt Hz	$70	10000 mW	1000 cm3

References:

Chaves, R. C.; Freitas, P. P.; Ocker, B.; Maass, W., 2008: MgO based picotesla field sensors, *J. Appl. Phys* **103**, 07E931-3.

Burnette, J. E.; et al., , 2008: Initial studies on micromechanical system flux concentrators, *J. Appl. Phys.***, 103**, 07E930-2.

Dong, S.; et al., 2005: Extremely low frequency response of magnetoelectric multilayer composites, *Appl. Phys. Lett*, **86**, 102901-3.

Dong, S.; et al., 2005: Push-pull mode magnetostrictive/piezoelectric laminate composite with an enhanced magnetoelectric voltage coefficient, *Appl. Phys. Lett.***, 87**, 62502-3.

Edelstein, A. S.; Fischer, G.A, 2002: Minimizing 1/*f* noise in magnetic sensors using a microelectromechanical system flux concentrator., *J. Appl. Phys.***, 91**, 7795-7797

Edelstein, A. S.; et al., 2006: Progress toward a thousandfold reduction in 1/*f* noise in magnetic sensors using an ac microelectromechanical system flux concentrator (invited), *J. Appl. Phys.***, 99**, 08B317/1-6.

Guedes, A.; et al., 2008: Hybrid - 3magnetoresistive/microelectromechanical devices for static field modulation and sensor 1/*f* noise cancellation *J. Appl.Phys.* 103, 07E924.

Jiang, L.; E.R.Nowak; Scott, P.; Johnson, J.; Slaughter, E. R.; Sun, 2004: Low-frequency magnetic and resistance noise in magnetic tunnel junctionsJ. J.; Dave, R. W., *Phys. Rev. B***, 69**, 054407-054415.

Parkin, S. S. P.; et al., 2004: Giant tunneling magnetoresistance at room temperature with MgO (100) tunnel barriers, *Nature Materials***, 3**, 862-867.

Schwindt, P. D. D., et al., 2004: Chip-scale atomic magnetometer, Appl. Phys. Lett., **85**, 6409.

Yuasa, S., 2004: Giant room temperature magnetoresistance in single-crystal Fe/MgO/Fe magnetic tunnel junctions, *Nature Materials*, **3**, 868-8